

Date of publication xxxx 00, 0000, date of current version xxxx 00, 0000.

Digital Object Identifier 10.1109/ACCESS.2017.DOI

Performance Evaluation of a Live Multi-site LTE Network

GEDIZ SEZGIN^{1,2}, YAGMUR COSKUN², ERTUGRUL BASAR³, (Senior Member, IEEE), and GUNES KARABULUT KURT², (Senior Member, IEEE)

¹Turkcell Iletisim Hizmetleri A.S., Istanbul, Turkey, gediz.sezgin@turkcell.com.tr

²Istanbul Technical University, Wireless Communication Research Laboratory (WCRL), Istanbul, Turkey, {coskuny, gkurt}@itu.edu.tr

³Department of Electrical and Electronics Engineering, Koç University, Sariyer 34450 Istanbul, Turkey, ebasar@ku.edu.tr

Corresponding author: Gunes Karabulut Kurt (e-mail: gkurt@itu.edu.tr).

ABSTRACT In this work, to quantify the field performance of a live Long Term Evolution (LTE) network, we design and implement a multi-layered performance monitoring system. This monitoring system delivers an accurate and thorough picture of the network behavior including switching, cellular, transmission, IP and data networks. The designed system enables measurement results gathered from different network layers and from both user and control planes through a mediation platform, paving the way for the collection of synchronous performance measurement results, including latency, handover ratios and throughput from network entities. Network performance metrics and the terminal-based measurement are jointly reported to reflect the subscriber perspective. Two field trials are conducted to highlight performance results of LTE networks, in a congested multi-cell with Release 12 support, and a sparsely populated cell with Release 14 support. Different multiple-input multiple-output (MIMO) configurations, including spatial multiplexing, transmit diversity, beamforming and 64×64 massive MIMO support, along with a selection of bandwidths and frequency bands are considered. The measurement results show that, without any significant latency cost, using more antenna elements provides higher user throughput, which also affects the overall cell throughput. However, doubling the number of antennas may not necessarily double the average data rates. Additionally, the average intrafrequency and interfrequency handover success ratios are observed to be acceptable, hence the changes among the selected the diversity and multiplexing technique does not have a visible deteriorating effect on the handover performance.

INDEX TERMS Beamforming, field tests, handover, latency, LTE network, massive MIMO field tests, spatial multiplexing, transmission mode, transmit diversity.

I. INTRODUCTION

Subscriber expectations from wireless networks are mainly dominated by the high data transmission rates. Mobile applications like video/audio streaming and online gaming demand such high rates, even under mobility conditions. In order to fulfill the rate requirements, Third Generation Partnership Project (3GPP) triggered the development of Long Term Evolution (LTE), starting with Release 8 (Rel-8). From the network deployment perspective, it can be clearly observed that LTE has been widely adopted. According to the report of GSA [1], globally 2.54 billion LTE subscriptions were recorded by the end of third quarter of 2017, and LTE networks account for 30.3% of total mobile subscriptions.

To address the high data rate expectations of subscribers, LTE standards make use of multiple-input multiple-output (MIMO) front-ends. The use of transmit diversity and mul-

tiplexing techniques, enabled through the presence of MIMO front-ends, can increase data rate and/or transmission reliability by tracking and adapting to different channel states [2]. Despite these advantages, it is important to note that there is a challenge introduced to mobile network service providers, by the use of the selected MIMO technique, determined according to the selected transmission mode (TM). MIMO techniques provide a higher performance in rich scattering channels, whereas conventional cellular networks ordinarily thrive under the line of sight (LoS) cases [3]. Furthermore, along with aiming rich scattering conditions and high signal to noise ratio (SNR) values, optimization of multi-path environments for MIMO is a must to achieve the desired data rates [4], [5].

The rank of the channel matrix, or the number of spatial layers of the wireless channel, is a critical element for the

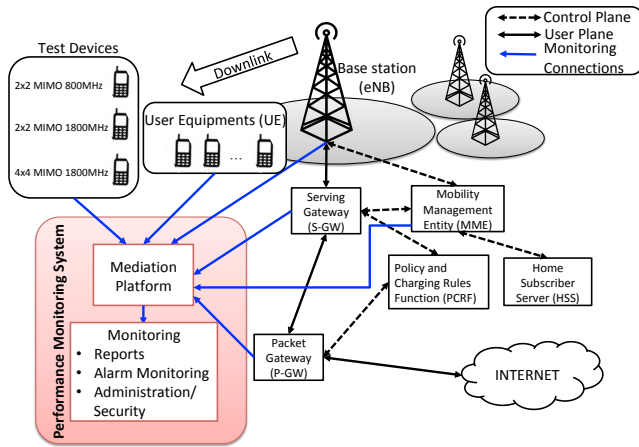


FIGURE 1: Simplified block diagram of the designed multi-layered performance monitoring system. Downlink data transmission rates, latency and handover ratios are jointly reported. Information from the control plane and the user plane are combined and performance metrics are monitored through the use of the mediation platform.

performance of MIMO-based systems, as higher rank values lead to higher transmission rates [6]. Through the use of multiple spatial layers, where multiple data streams are delivered on a given frequency-time resource, MIMO techniques are expected to linearly increase the transmission rates, with the number of antennas. The spatial layers are generated by the virtue of scattering and multipath platform between transmission and reception nodes.

Since directly affecting the system performance, MIMO transmission methods constitute an essential part of LTE networks. In this paper, we target to quantify the effect of the number of the antennas and the selected TM on live network performance from the subscriber perspective. With the goal of observing instantaneous performance metrics, we design and implement a multi-layered performance monitoring system. After gathering measurement reports from different network components, this system harmonizes and compiles the reports for performance evaluation and monitoring purposes. The simplified block diagram of the designed multi-layered performance monitoring system is shown in Fig. 1. To capture the network performance from the subscriber view, the impact of both the control plane and the user plane are incorporated. Measurements are captured from the mobility management entity (MME), serving gateway (S-GW), packet gateway (P-GW), base stations (eNodeBs, eNBs), and the user equipment (UE). The designed system is capable of jointly monitoring the transmission rates, latency and handover ratios.

Two extensive field trials are conducted using eNBs with Rel-12 and Rel-14 support. Different commercial UE types of distinct 3GPP terminal categories are camped to different frequency bands with different MIMO configurations. In the

first trial, we focus on the real-time performance of 2×2 and 4×4 MIMO techniques, where adaptive TM selection is applied in order to fit the system according to different radio conditions. This field trial environment is the extension of this basic configuration with 9 spatially spread eNBs, in a residential district in Istanbul during 8 weeks. The field trials address downlink (DL) performance and the frequency bandwidth for DL transmission are set as 10 MHz and 20 MHz for 800 MHz and 1800 MHz, respectively. In the second field trial, we use the designed multi-layered performance monitoring system to capture the performance of a Rel-14 eNB equipped with a 64×64 massive MIMO antenna. This configuration is shown to provide close to peak data rates, with a latency of less than 5 msec. To the best of our knowledge, our study is the first to present the performance of a live LTE network, under mobility conditions, incorporating 4×4 MIMO transmission in a densely populated network, also capturing the performance metrics of massive MIMO set-up in a live environment.

From our measurements, we observe that the considered MIMO techniques provide sufficiently high data rates and acceptable handover performance under highly loaded conditions. However, contrary to the ideal theoretical set-up, we observe that doubling the number of antennas may not necessarily double the data rates. Performance measurements are also discussed in terms of user experience, by taking the minimum requirements of different popular multimedia services such as video/audio streaming or online gaming into account.

This paper is organized as follows. In Section II, we present the related literature. In Section III, we provide an overview of the multi-antenna transmission methods supported in LTE standards. Section IV details UE restrictions and selected mobile application requirements to reflect the subscriber perspective. Details about the designed and implemented multi-layered performance monitoring system is given in Section V. In Section VI, field configurations are explained and field trial results are presented. Finally conclusions are drawn in Section VII.

II. RELATED LITERATURE

The theoretical performance analysis of the multi-carrier MIMO systems is already well established providing predictable outcomes for a given the channel model [2]. In addition to theoretical limits, practical performance limits of LTE Releases due to signaling channel allocations and predetermined signaling patterns, are also widely available in the literature [7], [8]. However, field test based performances are relatively scarce. Below we target to summarize the related literature that provides field measurement results.

3GPP LTE Rel-8 based field trials are conducted by Irmer et al., in [9]. The authors have focused on system level simulations and also performed laboratory tests for user throughput, spectral efficiency, and latency. Field trials of LTE Rel-8 are also presented in [10] in the 750 MHz band where the authors demonstrate a substantial throughput gain through

the use of MIMO techniques. A comprehensive analysis of user, cell, and radio link throughput performance statistics is considered in [11] by Buenestado *et al.*. Availability, accessibility, retainability, mobility, and integrity performance indicators are considered under different radio conditions. A literature review about LTE-Advanced based heterogeneous mobile network topological planning problem is presented in [12], with a high-level overview of system constraints. In [13], results obtained from a practical measurement campaign of an LTE network in a laboratory setup is given. A low complexity estimation technique is provided for the instantaneous throughput. Such a metric is beneficial in applications where the knowledge of throughput is critical.

One of the insightful works about conducting throughput, handover and latency tests in a 3GPP LTE frequency division duplexing (FDD) field trial is presented by Wylie-Green and Swensson in [14]. The authors measure DL and uplink (UL) throughputs for both single-user and multi-user scenarios. They also share handover success rates and average user plane latency values. Field tests show that block error rate (BLER) is inversely proportional to DL throughput under mobility conditions. In [15], simulations based on drive test measurements of are given. As will be shown in the following sections, their results reflect similar behavior to our measurements, where the average throughput is dependent on the user's location, and 4×4 MIMO usage leads to around 60% throughput improvement. Similar field performance comparisons are given in [16], and in [17]. The impact of the number of horizontally and vertically spaced transmit antennas for open-loop LTE configuration is reported in [18]. Field trials to investigate the performances of different MIMO techniques are reported in [19], however, the considered test network provides access only to test UEs, without serving a subscriber base.

In [20], various four and two antenna setups of an LTE system are tested under different antenna polarization, antenna spacing, rank, and TMs during a field trial in Kista. LoS and non-LoS (NLoS) performance comparisons with a UE specific 3D beamforming antenna are presented in [21] in an urban cellular testbed. User experience based performance results are compiled in [22] by Becker *et al.*, where the authors investigate the application level performance results by replicating the measurements in a wired access network to provide a reference for the wireless counterpart. Another field trial with spatially spread one macro and eight pico makes use of the Deutsche Telekom LTE network with Huawei. In [23], the authors have concluded that the coverage range varies between macro and pico sites for a better throughput performance. In [24], LTE system performance is evaluated for a high-velocity scenario, considering speeds up to 200 km/h. It is reported that although the velocity has an effect on the performance, its influence remains limited in the case when the signal-to-interference-plus-noise (SINR) coverage is well dimensioned. In [25], Brutyan presented a performance analysis of different MIMO modes in an LTE Rel-8 network. Another simulation study is given in [26],

investigating the performance analysis of LTE-A networks in different TMs using 16-ary quadrature amplitude modulation (16-QAM), considering fading channels with different antenna correlation conditions. Similarly, an open-loop and closed-loop TM comparison is presented in [27]. Around 2 dB theoretical performance gain is shown to be possible when an ideal closed-loop MIMO is used. The same topic is also analyzed in [28] by Mullner *et al.*, where the authors used the UE track analysis for a performance comparison. A fully loaded network system is simulated to illustrate that the open-loop fractional power control provides a higher throughput when the subscriber is near to the serving eNB. It is also noted that the performance declines when the subscriber moves closer to the cell edge. The authors suggest that maintaining a high throughput in such cases can be achieved by utilizing the closed-loop mode.

In [29], an RF planning tool based MIMO throughput prediction is presented. It must be noted that the simulation outcome may be different than the field trial measurements. Different antenna and modulation configurations are evaluated in [30], and the handover, delay, and end-to-end test topology performances are compared. A comparison between the predicted results and the field measurements is given in [31]. In [32], the use of massive MIMO technique is considered, however, channel measurements are used to estimate the rate improvement without the use of a live network.

One-way delay measurements of High Speed Packet Access (HSPA) and LTE networks with 2×2 MIMO antenna configuration are compared in [33]. [34] provides LTE MIMO performances in indoor environments, and compares the performances of MIMO TMs. [35] presents an outdoor MIMO throughput experiment by using a commercial LTE cellular network in 2.6 GHz band. 2×2 MIMO configuration throughput is measured in an urban area of Aalborg, Denmark in order to investigate the throughput performance by using the received signal strength indicator (RSSI) and the channel sounding data. Performance of an actual LTE network through drive tests is analyzed under mobile and stationary conditions in [36]. Voice and video transmission quality tests are reported in [37].

As summarized above, although MIMO utilization have been studied by considering different TMs and channel conditions, quantifying the effect of MIMO transmission under a fully loaded live multi-cell scenario, while jointly monitoring the data rates, latency and the handover ratios to fully reflect the subscriber experience, remains a gap in the current literature. This stands out as the main motivation of the current study.

III. MULTI-ANTENNA TECHNOLOGIES IN LTE

In general, multi antenna technologies are utilized for two main purposes; to increase the robustness of data transmission with transmit diversity or to increase data rate with spatial multiplexing (SM). In transmit diversity scenarios, the same data is transmitted redundantly over more than one

TABLE 1: Transmission modes.

Transmission Mode	Description
TM1	Single antenna transmission
TM2	Transmit diversity (open-loop)
TM3	Spatial multiplexing (open-loop)
TM4	Spatial multiplexing (closed-loop)
TM5	Multiuser MIMO
TM6	Transmit diversity (closed-loop)
TM7	Beamforming (with Massive MIMO support)
TM8	Dual layer beamforming (with Massive MIMO support)
TM9	Spatial multiplexing up to 8 layers

antenna, which increases the overall SNR at the receiver side. On the other hand, in SM scenarios, multiple separate streams of data are transmitted over multiple antennas, directly increasing the data rate in proportion to the number of antennas. Beamforming is another multi-antenna technology targeting to increase robustness, which uses multiple antennas to control the direction of a wavefront by appropriately weighting the magnitude and phase of individual antenna signals. Below, we detail the TMs of LTE.

A. TRANSMISSION MODES

Multiple antennas for reception and transmission at the eNB and in UE [38] are the key enablers of spatial plane. LTE standards support multi-antenna technologies that improve both link and system level performance in a wide range of scenarios. Transmitted data is mapped to layers after having been encoded and modulated. The number of transmitted layers is called the transmission rank. 3GPP LTE Rel-8 permits up to four layers to be transmitted in DL [39]. These layers are precoded and mapped to antenna ports in a procedure that is semi-statically configured to use one of seven TMs, shown in Table 1 [40]. In Rel-9 and Rel-10, additional modes, TM8 and TM9 are also introduced.

In LTE, different transmission scenarios are reflected in different TMs. TM1 uses a single transmit antenna whereas TM2, open-loop transmit diversity, is the default TM for MIMO in general. TM2 is used as the fallback option when SM modes are not available to be used due to the bad channel conditions. SM modes in LTE are TM3 (open-loop SM) and TM4 (closed-loop SM). TM3 supports SM of two to four layers, which are multiplexed to the transmit antennas without receiving any special feedback from the UE. To enable TM4, UE should report channel quality indicator (CQI), rank indicator (RI) and precoding matrix indicator (PMI) to the eNB as the feedback information.

TM2, TM3, and TM4 are referred to as single user (SU)-MIMO schemes. They are set for the configuration with two or four transmit antennas in DL. Transmission of multiple spatial layers up to four to a specified UE is possible using this mode. SU-MIMO scheme is applied to the Physical Downlink Shared Channel (PDSCH), which is responsible for transmission of information data in DL direction. The

maximum data rate that can be achieved by using SU-MIMO SM is 150 Mbps when the number of the transmit antennas is two, and 300 Mbps when the number is four.

The multiuser (MU)-MIMO scheme in TM5 allows allocation of different spatial layers to different users in the same time-frequency resource, and is supported in both UL and DL. In the UL, the eNB can always schedule more than one UE to transmit in the same time-frequency resource, which forms an MU-MIMO transmission configuration. However, in order for the eNB to be able to correctly differentiate and demodulate UE signals, eNB needs to assign orthogonal reference signals for UEs scheduled for the MU-MIMO transmission. For the distinction of multiple data in the same resource which are belong to various users, different cyclic shift values are assigned to UEs. For DL, if the configured TM is MU-MIMO, eNB can only schedule rank-1 transmission. Therefore in order to schedule more than one user, eNB has to employ different rank-1 precoding matrices regardless of the number of antennas. It is obvious that every UE only gets information about its own matrix. After decoding the information data with the help of the common reference signal and the precoding information gained from the control signaling, PMI/CQI feedback is constructed by the UE. However, nonoccurrence of this CQI report and the actual report can happen due to the fact that UE has no information about other UEs, including their interference levels.

TM6 is a special mode of closed-loop SM (TM4). In contrast to TM4, in TM6 only one layer is used, corresponding to a rank of one. The UE estimates the channel and sends the most suitable PMI to the eNB. TM7 and TM8 are beamforming modes with one or dual layers, respectively. Rel-10 has added TM9, in which up to eight layers can be used, so up to eight physical transmit antennas are required, this leads to up to 8×8 MIMO configurations. TM7 and TM8 also enable massive MIMO support, according to the capabilities of the antenna array. It should be noted that, during the field measurements in this study, TM2, TM3 and TM4 are the frequently used modes, along with TM7 and TM8 during the massive MIMO tests.

B. TRANSMIT DIVERSITY TECHNIQUES

For DL, the number of transmit antennas used in the configuration of the transmit diversity scheme could be two or four. It is possible to implement this scheme to all of the physical channels, which are PDSCH, Physical Broadcast Channel (PBCH), Physical Format Indicator Channel (PCFICH), Physical Downlink Control Channel (PDCCH), and Physical Hybrid ARQ Indicator Channel (PHICH). The only physical channel that other schemes can be carried out is PDSCH.

Since there is no distinct signal indicating the number of the transmitting antennas, blindly decoding the physical broadcast channel enables the UE to identify the number of the antennas, which could be one, two, or four. After the detection of that number, a suitable transmit diversity scheme

to the other physical channels is established. The well-known Alamouti code

$$B = \begin{bmatrix} S_0 & S_1 \\ -S_1^* & S_0^* \end{bmatrix} \quad (1)$$

provides the space frequency block code (SFBC), which is employed when the number of antennas is two [40]. Here $(\cdot)^*$ represents the complex conjugate, S_0 and S_1 represent the data symbols to be transmitted, and rows and columns stand for transmit antennas and frequency slots, respectively. The Alamouti code has been also postulated by standards [41] for the frequency domain as the basic transmit diversity MIMO mode. In this aforementioned mode, instead of employing two adjacent time slots, adjacent subcarriers are coded as pairs. An SFBC is more preferable for the high mobility scenarios since the orthogonality of the code could be spoiled when there is a fast changing channel.

The SFBC and frequency-switched transmit diversity (FSTD) are consolidated as [42],

$$B = \begin{bmatrix} S_0 & S_1 & 0 & 0 \\ 0 & 0 & S_2 & S_3 \\ -S_1^* & S_0^* & 0 & 0 \\ 0 & 0 & -S_2^* & S_3^* \end{bmatrix} \quad (2)$$

This is used with four transmit antennas in order to reduce the correlation between channels of several transmit antennas and to supply a simpler implementation of UE receivers. Unlike the previous situation, this transmit diversity scheme can be applied for all DL channels except PHICH.

The last remaining diversity scheme that is employed for PHICH has a different procedure when compared to the other schemes. First, a group of four subcarriers obtained by multiplexing four diversified ACK/NAK bits by utilizing orthogonal codes and a spreading factor of four. Three repetitions of that subcarrier group in the frequency domain provides frequency diversity gain and within each repetition. For the case of multiple PHICHs, employing different types is possible in order to have uniformly distributed power over transmit antennas of the base station [42].

C. SPATIAL MULTIPLEXING

The closed-loop and open-loop SM modes are the two modes used in SU-MIMO SM. For the closed-loop case in UL direction, in order to maintain matching of the transmitted signal and spatial channel perceived by the UE. The UE supplies a PMI to be used for performing spatial domain precoding on the transmitted signal. For DL direction, UE requires to feed the RI that specifies the maximum number of spatial layers can be supported in the current channel, the PMI and CQI in the UL that provides modulation scheme and channel coding rate that should be used in order to guarantee the block error probability at the UE to be below 10%, back to the eNB.

Codewords to layer mapping process differ according to type of SM. eNB's transmission rank schedule determines mapping of multiple codewords into multiple layers. For DL direction, hybrid automatic repeat request (HARQ) process

TABLE 2: Downlink physical layer parameter values set by the field UE-Category

UE Category	Maximum number of DL-SCH transport block bits received within a TTI	Maximum number of bits of a DL-SCH transport block received within a TTI	Total number of soft channel bits	Maximum number of supported layers for SM in DL
Cat 1	10296	10296	250368	1
Cat 2	51024	51024	1237248	2
Cat 3	102048	75376	1237248	2
Cat 4	150752	75376	1827072	2
Cat 5	299552	149776	3667200	4
Cat 11	603008	149776 (4 layers, 64QAM) 195816 (4 layers, 256QAM) 75376 (2 layers, 64QAM) 97896 (2 layers, 256QAM)	7308288	2 or 4

requiring ACK/NAK feedback on UL is enabled for every codeword. Therefore, even if there are more than two layers to be transmitted in DL, transmitting only up to two codewords is permitted in order to decrease the overhead due to the feedback requirement in the UL. The number of codewords depends on the number of layers.

The transmit precoding matrix indicator (TPMI) carries information about the used precoding matrix along with the DL control information. The length of the TPMI field depends on the number of the antennas, it has three bits if there are two antennas whereas it has six bits when there are four antennas. TPMI can also be used to enable frequency-selective precoding by avoiding DL signaling overhead by indicating that the precoding matrices from the last PMI report are utilized for their corresponding frequency resources [42].

If there is no trustable PMI feedback at the eNB, then the open-loop SM could be employed. This time the feedback consists of RI and CQI and the eNB states the transmission rank and a fixed set of precoding matrices that have an application in a cyclic manner to all subcarriers scheduled in the frequency domain.

IV. SUBSCRIBER PERSPECTIVE

In this section, we provide an overview of UE categories, their performance limits along with the data rate requirements of some popular applications.

A. UE CATEGORIES

In our measurements, cluster tests are realized with a Rel-10 compliant configuration. However, UEs supporting these specifications have not become reality by the equipment

TABLE 3: Uplink physical layer parameter values set by the field UE-Category

UE Category	Maximum number of bits of an UL-SCH transport block received within a TTI	Support for 64QAM in UL
Cat 1	5160	No
Cat 2	25456	No
Cat 3	51024	No
Cat 4	51024	No
Cat 5	75376	Yes
Cat 11	51024	No

TABLE 4: Video stream bit rate for different devices

De-vice	Cate-gory	Screen Resolution	Video		Bit Rate (kbps)
			High	Medium	Low
iPad		1024×768	4000	1280	480
iPhone	Cat 5,6,7,9 (depends on model)	320×480	800	256	96
Smart Phone	various cate-gories	320×240	400	28	48

manufacturers at the same speed. The root cause of this late recovery can be predicted from the economic perspective. Lower prices of chipsets directly affect the usage of new technology handsets by the subscribers. Slower development of terminals, compared to the network components, causes constraints in the system performance. As noted above, even though it is possible to observe 300 Mbps peak data rates for LTE networks with MIMO, the limitations stemming from terminals restrict the achievable peak throughput.

3GPP also develops standards for terminals that define their reception and transmission procedures, requirements, and the maximum capabilities according to their category. As standards are being developed, terminals become more capable of transmitting and receiving a higher number of bits. DL and UL physical layer parameter values for UEs are set by 3GPP in standard [43] and shown in Table 2 and in Table 3, respectively. As seen from Table 2, Transmission time interval (TTI) is 1 ms. During our measurements, we use Cat 4 and Cat 11 terminals. Additionally, since current commercial UEs support only up to 2 antennas, in order to test 4×4 MIMO configuration's performance, a specialized terminal that supports four antennas is used during measurements.

B. APPLICATION REQUIREMENTS

One main target for the evolution of mobile communication is to supply the possibility for significantly higher subscriber data rates. This includes targeting not only higher peak data rates but also higher data rates over the entire cell area, also including, subscribers at cell edges. The demand for

higher data rates stems from the increasing variety of mobile applications and data services. In order to properly evaluate the subscriber experience, and to be able to provide a comparison of the possibility of using different services and applications by users, the minimum requirements of popular mobile applications have been overviewed.

Video streaming is one of the most popular services. These services require varying data rates according to the video resolution and quality. [44] summarizes the associated requirements for different devices as given in Table 4. Specific video services like Youtube and Netflix recommend certain minimum bit rates. Youtube states that a minimum of 500 kbps of connection speed is required [45], whereas Netflix recommends a minimum of 1.5 Mbps of download speed for normal video quality and 5 Mbps for high definition (HD) video quality [46].

Video conference applications are another popular applications. Skype recommends 0.1 Mbps download and 0.1 Mbps upload rate for voice calls, 0.5 Mbps download and 0.5 Mbps upload rate for video calls and 1.5 Mbps download and 1.5 Mbps upload for HD video calls [47]. For audio streaming applications like Spotify, a minimum of 0.15 Mbps download data rate is recommended. Video games, which are one of the most downloaded applications for mobile terminals, lower delay is more important than higher data rates. As an average, a minimum of 10 Mbps data rate and a maximum of 10 ms of latency can be tolerated for providing a desirable online gaming experience [48].

Even when the system performance meets the application requirements listed above, another limiting factor which prevents applications from functioning properly could be the UE's category. The maximum rates, which UEs can provide according to their category, are listed in Tables 2 and 3. When this information is taken into account, it can be seen that some categories of UEs cannot allow using all applications or data services. For example, high-quality online gaming may not be possible for Cat 1 UEs that can only provide maximum 10 Mbps data rate.

V. PERFORMANCE MONITORING SYSTEM

The designed and implemented multi-layered performance monitoring system delivers an accurate and thorough picture of network behavior including switching, cellular, transmission, IP and data networks. Together with counters received from network elements, interpolated data can be used in calculations and aggregation, and appear in reports. These tools include the capabilities to view threshold-based alarms and KPIs in the form of reports or drill down to the raw data as received from the network. Performance management allows the user to run special period calculations to find the most, or least, busy time intervals of a day, or other time intervals based on the data that was accumulated by the performance management module (PMM). PMM also generates key performance indicators (KPIs) and key quality indicators (KQIs) based on network elements (NE) counters, Transaction Data Records (TDRs), NEs event-based statistics

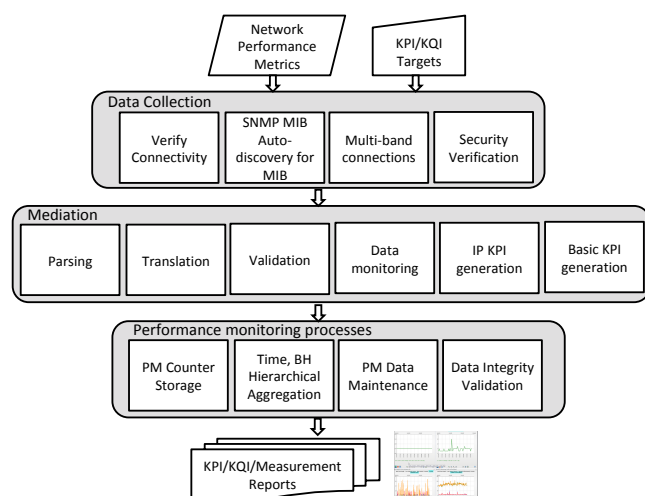


FIGURE 2: An overview of the process flow of the multi-layered performance monitoring system. Data collection is performed through the connections given in Fig. 1 in a release agnostic manner. Both test and real-time UE can be monitored. Mediation process is followed by the performance monitoring steps in the database. The outputs can be processed according to the target KPI/KQI values, that can also be defined as an input to the performance monitoring system. Further connections with the administrative and security processes are also supported with the designed system.

and traditional billing xDataRecords (xDRs), providing a clear insight into network and service performance. It performs the process of normalization (mapping the raw data into one generic format, which can then be used by the system regardless of the original equipment format), aggregation of the data, late and missing counters calculations and traffic analysis calculation (such as busy hour and peak hour).

This monitoring system enables measurement results gathered from different network layers and from both user and control planes to be reported and evaluated. Measurements are based on two way active measurement protocol between eNB and Enhanced Packet Core (EPC), that supplies two-way or round-trip measurements (TWAMP) instead of unidirectional capabilities. Measurement results, including latency, handover ratios and DL throughput, have been collected from network entities including eNBs, MME, S-GW, P-GW, and the UE. Measurements are collected as bulk data in the measurement reports and then harmonized to obtain target period calculations. Latency measurements are captured through sending ping requests from the eNB to network data center, located at a close proximity to the MME. Time difference between session sender (eNB) and the reflector mode (EPC) is defined as the user plane latency, which is based on the network architecture design. The user plane latency mainly affects the user experience in latency based applications' performances, like online gaming, and real-time video sharing.

Our multi-layered performance monitoring system gathers logs from different network components that are then harmonized and compiled for evaluation of the performance from subscriber aspects. The designed monitoring system, shown in Fig. 1, includes different network components. To capture the network performance from a realistic perspective, as monitored by the subscriber, the impact of both the control plane and the user plane are monitored, through the use of a mediation platform. The designed and implemented mediation platform provides a bidirectional connectivity to any network element, element managers, sub-network management systems. Mediation delivers a single platform for the management of connectivity, collection and initial processing of network management data including faults alarms, performance indicators and xDRs. This platform can connect, collect and process performance data from the network equipment using multi protocols and file formats such as SNMP and FTP. Here, the data is parsed, translated, validated, monitored and target KPIs are generated. This mediation layer stores the data in a temporary repository and then sends the results to the upper layer applications through various standard APIs. The mediation platform then yields to the performance monitoring tasks that enables processing of the collected data regardless of the equipment types that they were generated from. An overview of the process flow is shown in Fig. 2.

Unlike other field measurement studies, in order to obtain an accurate picture of network behavior and performance counters received from network elements are merged with aggregation reports since these tools include the capabilities to view threshold-based alarms and KPIs in the form of reports or drill down to the raw data as received from the network. The designed performance monitoring system allows the user to run special period calculations to find the most, or least, busy time intervals of a day, or other time intervals based on the data that was accumulated by the monitoring system.

The monitoring system is responsible from the selection and the classification of measurement data, and it provides a sequential raw data stream according to required performance metrics based on time, location, eNB, terminal, and subscriber. Blank numerals, on the order of 10^9 are converted to data sequences according to the target requirements.

VI. FIELD TRIALS

The main objective of the field trials is to measure the relative performance of different antenna configurations at the eNBs and the UE. The field trials are conducted in residential districts in Istanbul and Ankara, in Turkey. LTE eNBs with Rel-12 features are tested in Istanbul. An LTE eNB with Rel-14 features, supporting a 64×64 Massive MIMO antenna with 64 independent RF channels, is used during the tests in Ankara.

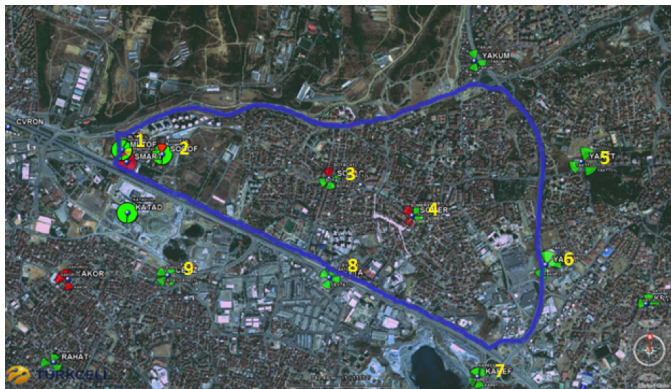


FIGURE 3: The drive routes in cluster. A residential district in Istanbul, Turkey is considered. Cite labels and eNB locations are represented on the map. Measurements are taken during live traffic, spanning eight weeks.

TABLE 5: Cell configurations.

Site	Number of Sectors	Frequency Bands
Site-1	4	800, 1800
Site-2	3	800, 1800
Site-3	4	800, 1800
Site-4	4	800, 1800
Site-5	3	800, 1800
Site-6	3	800, 1800
Site-7	4	800, 1800
Site-8	4	800, 1800
Site-9	3	800, 1800

A. FIELD TRIALS WITH REL-12 BASE STATIONS

The UE is driven along routes in the selected cluster of nine eNBs at speeds ranging from 20-60 km/h. Fig. 3 shows an aerial photograph of the area with drive routes drawn in. The selected cluster contains business areas, residential areas, and dense-main road coverage. Average site to site distance of the given cluster is approximately 1.3 km.

Two of the sites serve to business areas, one of the sites is suburban with flat, open areas and relatively low buildings. Three sites serve urban, dense and relatively high buildings. The remaining four sites serve dense main roads. Site-based basic configurations are given in Table 5. Test setup parameters are summarized in Table 6. Sites are designed as three or four sector configurations, and the sectors aim to improve coverage. When the traffic density is higher, more layers are activated for the given sector/site.

Field measurements are performed using the commercial UEs, which support 2×2 and up to 4×4 ([number of transmit antennas] \times [number of receive antennas]) MIMO transmission. Samsung S5, Samsung Galaxy Note 4, and Huawei 4 \times 4 B618s-22d WTTx modem are used for 800 MHz 2×2 , 1800 MHz 2×2 , and 1800 MHz 4×4 , respectively. Samsung S5 and Galaxy Note 4 terminals are classified as UE Cat 4. Huawei WTTx modem is classified as UE Cat 11. Cat 4 terminals ideally support 150 Mbps DL throughput and 50 Mbps UL throughput, as noted in

TABLE 6: Basic parameters for test setup.

Parameter	Description		
Carrier Frequency	800 MHz	1800 MHz	1800 MHz
System Bandwidth	10 MHz	20 MHz	20 MHz
UE Conditions	UE always scheduled over entire bandwidth by fixing the given frequency		
Number of Antennas (eNB)	2	2	4
eNB Antenna Gain	15.4 dBi	17.4 dBi	17.4 dBi
Number of Antennas (UE)	2	2	4
LTE Duplex Mode	FDD		
eNB Output Power	2×43 dBm	2×44.7 dBm	4×44.7 dBm
RS Power Boost	+3 dB	0 dB	0 dB

Table 2 and Table 3. Cat 11 terminal supports 600 Mbps DL throughput and 50 Mbps UL throughput. The trials address DL performance only, the bandwidth is set as 10 MHz and 20 MHz for 800 MHz and 1800 MHz, respectively.

In the mobility scenario, cell reselection and handover decisions are based on Reference Signal Received Power (RSRP), which is a cell-specific signal strength related metric. Similar to the RSRP measurements, Reference Signal Received Quality (RSRQ) measurements are used mainly to provide ranking among different candidate cells in accordance with their signal quality. This metric can be employed as an input in making cell reselection and handover decisions, where the RSRP measurements are not sufficient to make reliable decisions. Slow handover process is used in the test network.

In order to have measurement results that reflect the normal performance of the network, under the commercial LTE traffic, the power setting of each site is kept unchanged during the tests. LTE specification does not define DL power control directly, but the procedure consists of several elements such as Reference Signal, PDCCH, and PDSCH. During the field trial, TCP protocol is used with acknowledged mode (AM), because of the commercial traffic that is being carried during the cluster tests. PDCP and RLC packet lengths are defined as given in 3GPP TS 36.323 and 36.322, respectively. Also, discontinuous reception is activated during the trials.

For the given cluster, each eNB is set with similar carrier configurations. The number of sectors may change based on the coverage target. Layer management for the LTE sites are towards the lower frequency bands, since lower frequencies are subject to better propagation conditions. Therefore if the subscriber has favorable radio conditions and is not so far from the cell center, then layer management function pushes this subscriber to keep the 1800 MHz frequency band, depending on the site configuration. If the cell load is increased and if the subscriber mobility is from the cell center to the cell edge, then lower frequency bands like 800 MHz are used. Although subscribers are pushed to lower frequency bands when they are moving from the cell center to the cell edge, handover between sectors can be realized both at 800 MHz and 1800 MHz, due to the site to site distances. If the site to site distance is low, then handover between two sectors can

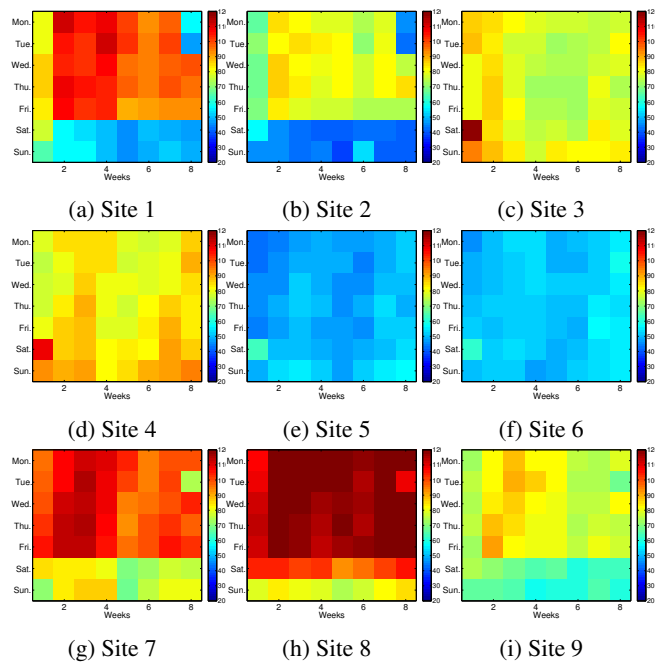


FIGURE 4: Average number of users.

be from the source 1800 MHz frequency to the target 1800 MHz frequency.

The scheduler is in charge of assigning bandwidth resources to UEs and deciding on how channels in both directions are utilized by the eNB and users of a cell. Hence, necessary Quality of Service (QoS) for UE connections per sub-frame level (i.e. each 1 ms TTI) is enforced. eNBs under the given cluster have the same scheduling type (proportional fair). The eNB site installation is designed to mimic a conventional macro cellular site with antennas above the rooftop height.

Each eNB antenna enclosure houses four linearly arranged columns with a horizontal spacing of 0.7λ ($\sim 8\text{cm}$). Each column consists of a dual-polarized (+45 and -45 degrees), co-localized antenna pair. In total, there are eight antenna ports per enclosure. Each sector has either single or two separate antenna enclosures mounted on horizontal bars and inter-antenna spacing around 20 to 30 cm. The eNB is equipped with a dynamic calibration system that ensures coherent transmission from the antennas. On the other hand, UE antennas are internal as originally used for commercial purposes. UE is mounted on the glove of the van.

For the backhaul point of view, all sites have fiber backhaul, which supports up to 1 Gbps symmetric speeds. This capacity does not constitute a primary bottleneck for the subscriber throughput degradation.

Field trials with Rel-12 eNBs aim to measure the relative performances of different antenna setups at the UE and the eNB sites. Drive tests along the cluster are divided into three subgroups, which are 800 MHz 2×2 MIMO, 1800 MHz 2×2 MIMO and 1800 MHz 4×4 MIMO, addressing to evaluate DL performance. In addition to drive tests, the

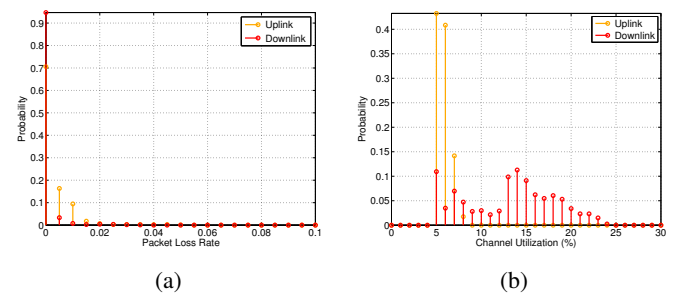


FIGURE 5: Histogram of performance metrics. (a) Packet loss rate (b) Channel utilization.

average metrics of the nine sites are captured during an eight week period. We target to observe the effect of throughput changes in case of;

- Low (800 MHz) versus high (1800 MHz) frequency bands: As the nature of path loss, on the average lower frequency signals are subject to lower attenuation levels than the high frequency signals, as the UE is going away from the eNB to the cell border.
- 10 MHz bandwidth versus 20 MHz bandwidth: Increased number of resource blocks results in increased user throughput under similar radio conditions.
- 2×2 MIMO and 4×4 MIMO in the same frequency band: To take advantage of the spectral efficiency, higher order MIMO front-ends always serve higher throughput opportunities. However, the improvement in the throughput may be lower than the theoretical expectations.

Cluster test is driven along with the commercial traffic, and all tests are taken under the multi-user environments in a live network from nine distinct cell sites. During the tests, the practical peak throughput shared among the number of active users is reported, which is proportional to their signal quality. Fig. 4 shows the average number of connected user distributions over the time for each site. Packet loss rate and the channel utilization histograms are given in Fig.5. Accordingly, a minimum of approximately 5% channel utilization is observed due to the presence of cyclic prefix portions of OFDM symbols, with an average UL (DL) packet loss rate of 0.0008 (0.0032). We can observe that the sites are operating under the medium-heavy loaded traffic. It is clear that tests are performed under the real network conditions, and the absolute performance may change for different traffic densities.

DL throughput on PDSCH directly depends on the CQI value reported by the UE according to channel conditions. Modulation coding scheme (MCS) values corresponding to CQI values are adjusted by the system itself. However, modulation order versus MCS value is defined by TS 36.213 [49]. Although there have been lots of enhancements in the LTE physical layer, yet higher order modulation schemes were not introduced in the specification until Rel-12, which includes a table for determining MCS versus modulation

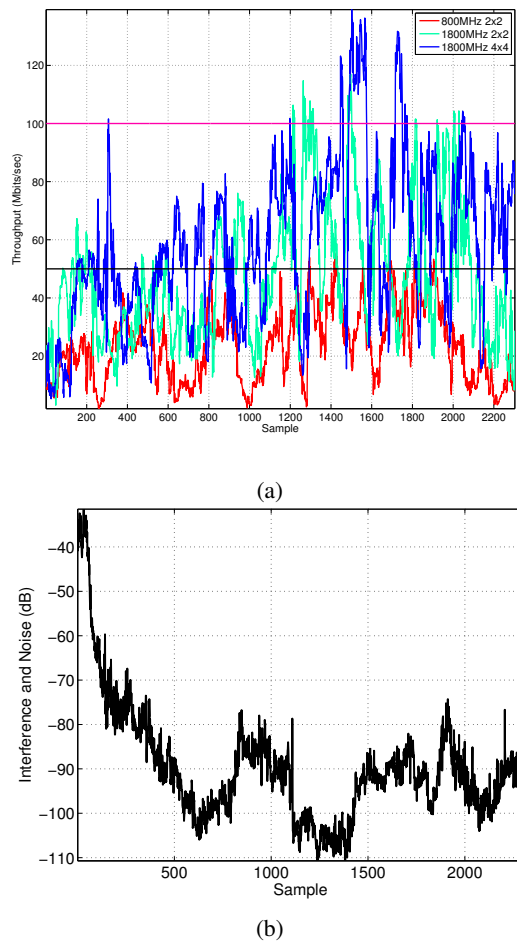


FIGURE 6: Field measurements. (a) Throughput (b) Interference.

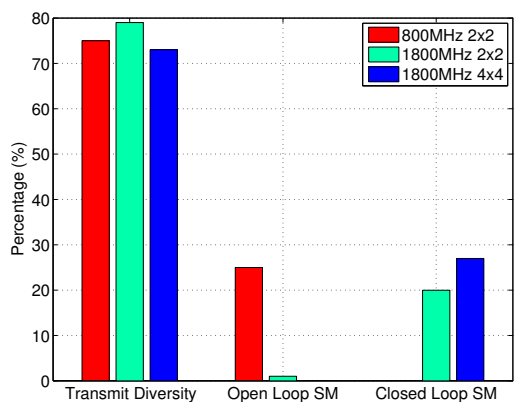


FIGURE 7: Usage rates of multi-antenna techniques in terms of transmission modes.

order. A new table for higher order modulation schemes is introduced in the 3GPP standard in Rel-12, aiming to enhance the spectral efficiency of the system and increase the peak data rates. Table 7 shows the CQI vs MCS mapping compiled from Rel-12 with suitable modulation under the

TABLE 7: CQI vs MCS mapping and observation ratios.

CQI	MCS	Modulation	Observation ratio (%)
4	8	QPSK or 16QAM	0.62
5	9	QPSK or 16QAM	4.62
6	10	16QAM	1.74
7	13	16QAM or 64 QAM	1.91
8	14	16QAM or 64 QAM	7.87
9	17	64 QAM	10.64
10	16	16QAM or 64 QAM	27.91
11	19	64 QAM	11.51
12	20	64 QAM or 256 QAM	14.27
13	20	64 QAM or 256 QAM	13.34
14	21	64 QAM or 256 QAM	1.45
15	21	64 QAM or 256 QAM	4.13

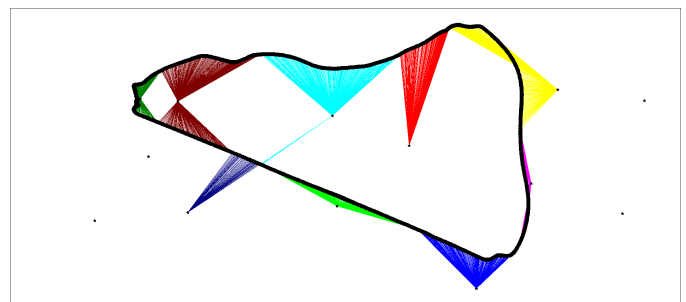


FIGURE 8: Best server cell connection to UE for the test route.

real-time traffic measurements, along with the observation ratios. During tests, CQI is reported between 4 and 15. It is clearly seen from the table below that, CQI=10 is the most frequently reported CQI. Also, 64-QAM CQI's are reported around 73%, which means the radio conditions of the given cluster are considerably good. On the other hand 16-QAM CQI ratio is around 20%, and the remaining 7% CQI belongs to quadrature phase shift keying (QPSK) modulation.

Fig. 8 is used for interference calculations. Different colors define different server cells, which are connected to the test UEs for the given route. Fig. 6 (a) shows the DL throughput results of different frequency, bandwidth and MIMO configurations. It is clearly seen that the increased spectral efficiency or modulation order, which is determined by the MCS value corresponding to the reported CQI, directly affects the DL throughput level. Also, the wider bandwidth results in a higher DL throughput. During the cluster tests, a maximum 55.3 Mbps DL throughput is reported with 800 MHz 2×2 MIMO configuration. In the 1800 MHz configuration, 117 Mbps and 139.2 Mbps peak throughput values are measured for 2×2 MIMO and 4×4 MIMO cases, respectively. It is also important to remind that the tests are performed under real traffic conditions. Other legacy user effects should also be considered. The gap between the trends at 2×2 and 4×4 MIMO configurations in the same frequency and bandwidth conditions explains the gain of the spectral diversity usage, which is around 17%. As noted before, tests are executed with Cat 4 and Cat 11 terminals. Experienced throughput

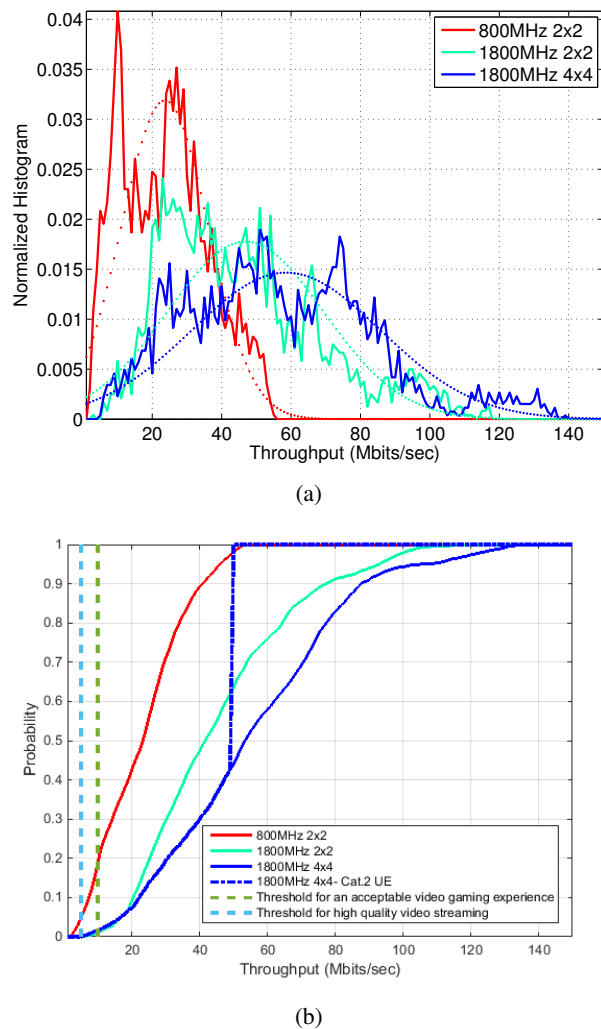


FIGURE 9: Throughput measurements. (a) Histogram and their maximum likelihood normal distribution fits (dashed lines) (b) cdf.

values do not only depend on network configuration, but also on the UE category. The interference level in all bands are measured through the use of a Ascom TEMS tool, and the interference level measurements are shown in Fig. 6 (b). In this plot, interference level is also shared as the secondary axis. It is clearly seen that lower interference level results in higher data throughput for all frequency and bandwidth combinations. System link budget is designed to dedicate enough overlaps between the neighbor sites, which do not decrease the cell edge performance dramatically.

Even though the maximum throughput of the 4×4 MIMO configuration is theoretically expected to be two times higher than the 2×2 MIMO configuration with the same bandwidth, the results imply that achieving the maximum throughput in a live network is relatively difficult. The selected TM is one of the most important reasons why the maximum theoretical throughput cannot be achieved in a commercial network under non-ideal propagation conditions. Fig. 7, reporting the

usage of UE TM, shows that the network chooses the transmit diversity mode, which cannot offer a doubled throughput like the SM mode, in order to compensate channel conditions and to reduce the number retransmissions. TM2 is the most reported TM, which is expected because the terminals are mobile and channel propagation conditions were not good. It is clearly seen that 1800 MHz 4×4 MIMO UE reports more TM4 mode usages than other UEs. This will directly affect the performance improvement of the 4×4 configuration. Moreover, there is no TM4 reported by UE for 800 MHz 2×2 MIMO configuration because this feature is disabled by the vendor. Network radio infrastructure used during the tests are acquired from Ericsson and the 800 MHz 2×2 radio module design does not support TM4 due to the link budget based constraints.

In order to have the distribution of each configuration, probability functions are collected. In Figs. 9 (a) and (b), the probability density function (pdf) and the cumulative density function (cdf) estimates based on empirical histograms of different configurations are shown, respectively. 1800 MHz 4×4 MIMO configuration aims to serve higher DL throughput than other configurations. In Fig. 9 (a) the peak normalized histograms are around 8, 22, and 77 Mbps for 800 MHz 2×2 , 1800 MHz 2×2 , and 1800 MHz 4×4 configurations. However, 50% probability in cdf plots (Fig. 9 (b)) are the average throughput values for the given configurations. From this figure, it can be clearly seen that the samples of higher throughput is always collected with 4×4 MIMO configuration, for all radio conditions. However, when a normal distribution is used to fit the empirical histograms, the actual behavior of the throughput of different configurations becomes more apparent. The average throughput values are estimated as 23.6298 Mbps, 46.8550 Mbps, 58.5848 Mbps and standard deviations are 12.5139, 22.4663 7.2139 for 800 MHz 2×2 , 1800 MHz 2×2 and 1800 MHz 4×4 configurations, respectively. Theoretically, the throughput of the 4×4 MIMO configuration is expected to provide double the 2×2 configuration's average throughput. This study demonstrates that even though network throughput is expected to be directly proportional to the number of spatial planes, it cannot be observed in the real networks due to application problems of multi-antenna technologies. This implies that the MIMO technology cannot be used with its true potential for throughput.

From the subscriber experience perspective of this network cluster, the collected data from measurements are evaluated using the information provided in Section IV. Applications besides high-quality video streaming and online video gaming can be smoothly supported by the system with all of those configurations, only high-quality video streaming and online video gaming data rate requirements are considered, and their thresholds are included in the figure. From Fig. 9 (a) it can be observed that, the 5 Mbps data rate requirement of HD video quality can be supported by 95% of the users for the 800 MHz 2×2 MIMO configuration and, more than 99% of the users for 1800 MHz 2×2 and 1800 MHz 4×4 configurations.

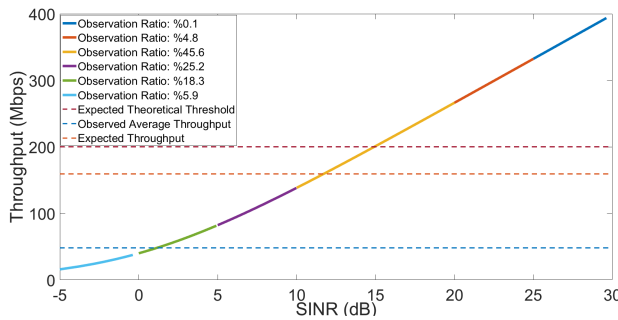


FIGURE 10: Throughput analysis for 1800 MHz 2x2 MIMO configuration.

Additionally, the 10 Mbps data rate requirement of video gaming can be supported by 81% of the users for the 800 MHz 2x2 MIMO configuration and, 98% of the users for 1800 MHz 2×2 and 1800 MHz 4×4 configurations.

Before completing assessments about throughput measurements of this study, we would like to give a short review about theoretical expectations versus real system performance using detailed logs from 1800 MHz 2x2 MIMO configuration, as shown in Fig. 10. Observation ratios of different modulation orders and various measured SINR ranges were mainly used to calculate theoretical capacity and expected throughput values. First, the expected value of throughput for this specific configuration is evaluated as 200 Mbps. Moreover, the famous capacity formula is used to calculate the expected capacity of the system

$$C = \min(N_T, N_R)B \log_2(1 + \text{SINR}) \text{ [bits/sec]}, \quad (3)$$

where N_T (N_R) represents the number of transmit (receive) antennas and B represents the system bandwidth. It is calculated as 159 Mbps for SM TM of 2×2 MIMO configuration, when the observation ratios of SINR ranges are taken into account. Since the mean value of measured throughput was around 50 Mbps, it can be concluded that the system is working far below its true potential.

Average user plane latency for given cluster is around 6.1 msec, and site-based distribution over the time is given in Fig. 11. The latency histograms are shown in Fig. 12. The standard deviation of latency measurements per site changes between 0.21 to 0.79 msec. Half of TWAMP value is shared as one way latency, and we can see from these heat maps showing measured latency that latency do not directly affect the user throughput performance. In order to convert the distributed architecture to centralized one, it is recommended by Ericsson to decrease latency to less than 5 msec [50]. However, from Fig. 12 it can be observed that this recommendation is not always satisfied.

Mobility and intrafrequency handover success rates are taken for the handoff performance. The interfrequency-based handoff performance is not shown since neighboring between sites is only intrafrequency based. This implies that, according to system design, it is allowed to handoff only to the

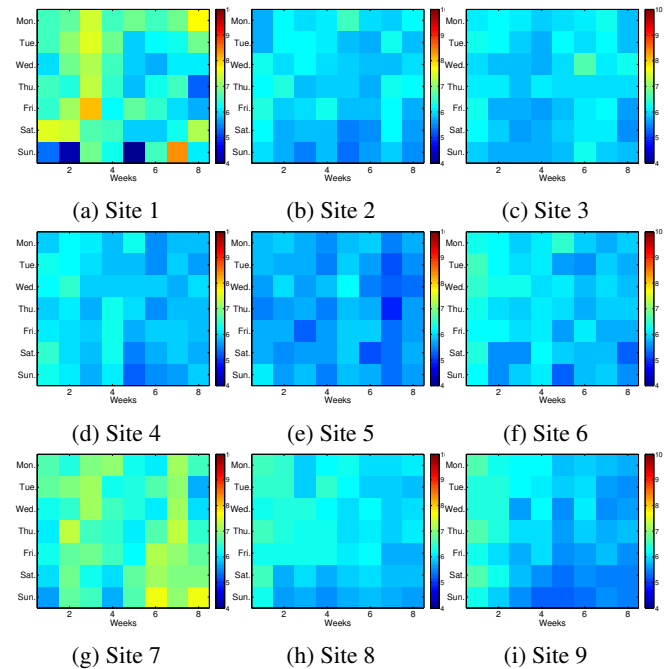


FIGURE 11: Average latency (milliseconds).

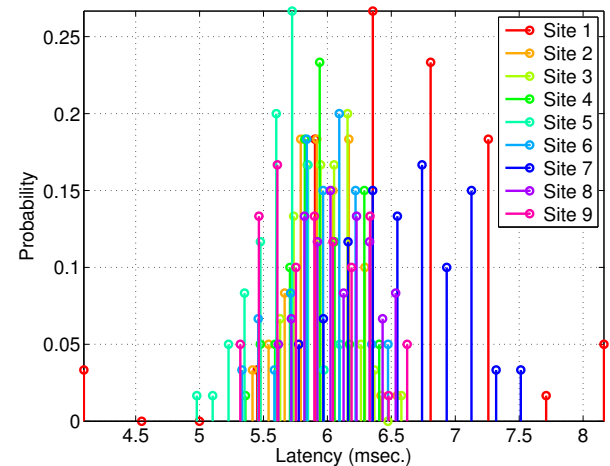


FIGURE 12: Histograms of latency per site.

same frequency at the target cell. In Fig. 13, intrafrequency performance of sites are plotted. In site 7, it can be observed that although the number of users is high, intrafrequency handoff success rate is considerably low. On the other hand, inter frequency handover is observed mainly in the pedestrian scenarios, which is given below Fig. 14. In order to trigger interfrequency handover within the sector, load balancing mechanism needs to be properly functioning. This is almost perfect at site 1, where some deployment necessity is needed at site 7. It is seen that both intra and inter frequency handoff cases, performance results converge to 100%. Intra-frequency handoff success rates are more stable than inter-frequency handoff cases. Handover scenarios for different

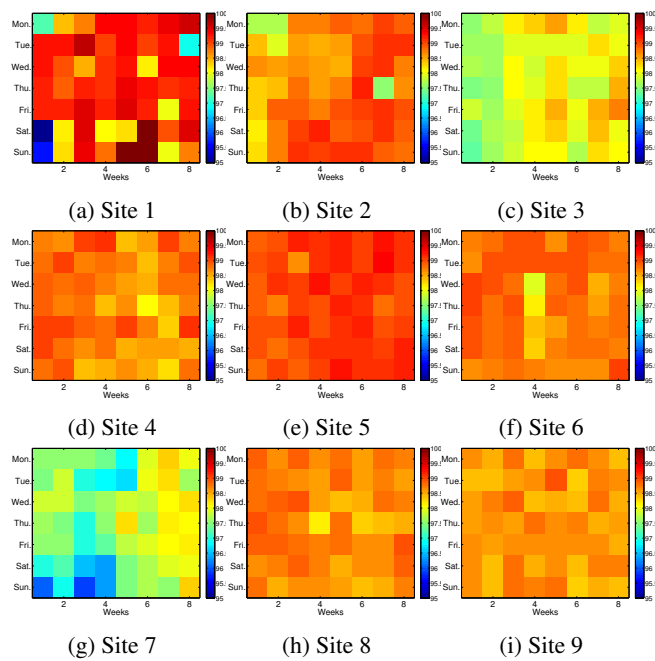


FIGURE 13: Average intrafrequency handover success rates (%).

MIMO configurations belong to the same flow. For a single connection scenario, Radio Resource Control (RRC) connection is linked to a single baseband module. Considering the following releases that support inter baseband carrier aggregation, behavior of handover scenarios may change according to radio conditions.

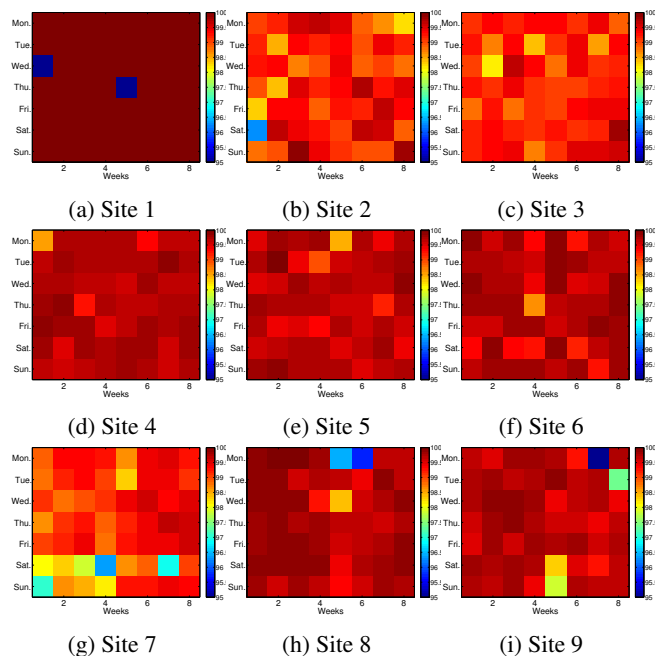


FIGURE 14: Average interfrequency handover success rates (%).

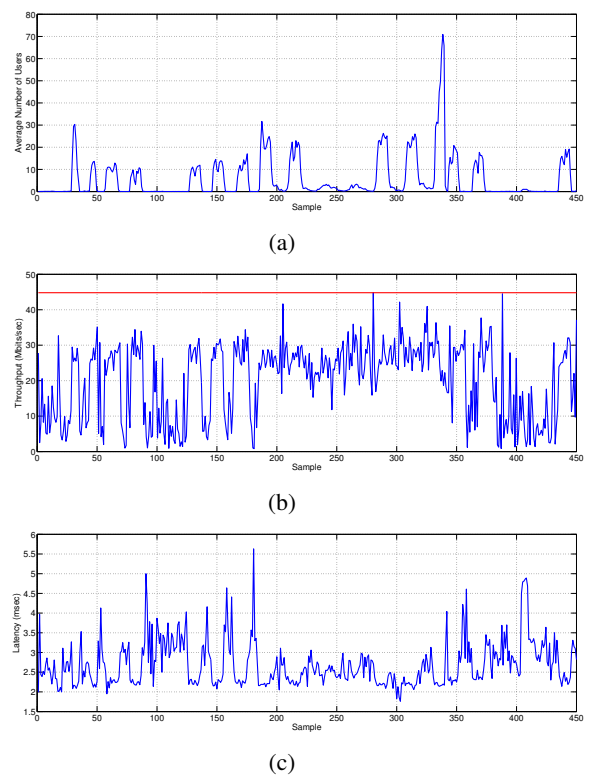


FIGURE 15: Massive MIMO antenna supported measurements. (a) Channel utilization (b) Average throughput (the maximum achievable throughput is also indicated with solid red line), (c) Latency.

B. FIELD TRIALS WITH REL-14 BASE STATION

The designed multi-layered performance monitoring system can work with all LTE releases, and can be used to monitor the performance of the live network in accordance with the determined system configuration. In this subsection, we provide measurements from an eNB with Rel-14 features.

As noted above, MIMO techniques are used to dramatically increase radio performance by using multiple antennas at the transmitter and receiver. The spectral efficiency increases as the total power distributed between the antennas. Although current MIMO techniques actively used in cellular systems today are mainly designed to increase the user data speeds, ongoing MIMO standardization studies for 5G systems have goals to substantially increase total data speed or system capacity in a service area. As a useful approach, increasing the number of antenna elements, can significantly aid to attain the target performance goals, supported through the massive MIMO techniques. As a result, 3GPP is considering further integration of massive MIMO techniques in the standards, early versions TM7. Pre-commercial stage MIMO systems are also available with 3GPP TS36.141 and ETSI EN 300019-1-4 support [51].

In massive MIMO antenna technology adaptive beamforming technique used and the system requires DL TM7 or higher. Processing of DL user-specific signals transmitted

is required. A specific beam can follow a user in mobility in a range dynamically. As TDD systems use the same frequency range both for UL and for DL, it is more suitable for massive MIMO applications. In order to achieve accurate beamforming, which implies getting proper beamforming weight for users, it is important to obtain precise and rapid channel estimation. Since TDD systems use same frequency band for both UL and DL, the UL signals of the users can be exploited by eNBs for DL channel estimation.

The 64×64 massive MIMO antenna used during tests has served on 10 MHz frequency bandwidth in 2600 MHz band (B38) with a maximum of 16 streams. eNB output power is set to 50.8 dBm. 64-QAM constellation is supported with a total of 600 subcarriers. 2 antenna UEs are supported. A total of 8400 resource elements are available. In this configuration, without the reference signals, 46.872 Mbits/sec is achievable. However, signaling redundancy must also be considered in the peak throughput calculations. 10% of the band is allocated to PDCCH. A cyclic prefix of 6.6% is used. An additional 19% of the band is used for reference signals. Theoretical maximum data rate that can be achieved on 10 MHz bandwidth in TDD system in presence of reference signals becomes 30.157 Mbits/sec. Our field tests were configured according to DL/UL ratio of 3/1 and special sub-frame ratio of 10:2:2. Hence the maximum data rate per beam becomes 22.402 Mbits/sec.

Measurements are collected from a single cell over 5 days through the performance monitoring system. Average number of users are shown in Fig. 15 (a). Note that this site is operating over 2600 MHz and operated at a low congestion level for trial purposes. The throughput levels are shown in Fig. 15 (b) along with the maximum two beam throughput shown in red. Latency values are shown in Fig. 15 (c), indicating an average latency of 2.69 msec. Regarding the handover performances a success rate of 100% is reported throughout the test duration.

The field tests were configured to support both TM7 and TM8, hence providing a maximum of 44.804 Mbits/sec. However, 358.432 Mbits/sec is achievable by using 16 simultaneous beams. Note that approximately 88 Mbits/sec is possible with 4×4 TDD system with 10 MHz bandwidth, hence the potential of massive MIMO systems are clear. Despite a higher processing complexity due to beamforming weight calculations and tracking of active users, there are no disadvantages observed from the latency measurements with the probability of a less than 5 msec latency is supported 99.77%, satisfying the subscriber expectations [50]. As a result, massive MIMO technology, which is one of the enabling technologies for the 5G New Radio, is expected to provide a significant throughput increase with a high quality-of-service.

VII. CONCLUSION

In order to investigate the performance of LTE networks from the subscriber perspective, we have designed and implemented a multi-layered performance monitoring system.

This system enabled us to conduct comprehensive field tests. In this work, we have presented the impact of MIMO configurations and the carrier frequencies along with the allocated bandwidth on the performance of LTE networks through the use of the performance monitoring platform. Field trial results of two measurement campaigns targeting Rel-12 and Rel-14 networks.

By quantifying the performance of different MIMO TMs, we have observed that interference levels directly affect the system performance. The lower interference results in a higher order of TMs, which leads to increased throughput. Also, as expected, MIMO antenna configurations affect the throughput, however not in the same order as the number of used antenna elements, while a significant improvement is observed with the use of massive MIMO support. The latency measurements have been observed around 6 milliseconds, depending on the congestion level of traffic utilization, with almost 100% handover success rates. For the future work, we target to focus on the performance of LTE networks under HetNet scenarios, which include pico, femto and micro stations. Furthermore, application layer performance based on packet tracing is targeted.

REFERENCES

- [1] GSA, "LTE Ecosystem Snapshot," Tech. Rep., Feb, 2018.
- [2] D. Tse and P. Viswanath, Fundamentals of wireless communication. Cambridge university press, 2005.
- [3] S. Adhikari, "Critical analysis of multi-antenna systems in the LTE downlink," in IEEE Int. Conf. on Internet Multimedia Services Architecture and Applications (IMSAA), 2009, pp. 1–6.
- [4] C. Studer and E. G. Larsson, "PAR-aware large-scale multi-user MIMO-OFDM downlink," IEEE J. Sel. Areas Commun., vol. 31, no. 2, pp. 303–313, 2013.
- [5] D. Tse and P. Viswanath, Fundamentals of wireless communication. Cambridge University Press, 2005.
- [6] B. Karakaya, H. Arslan, and H. A. Cirpan, "Channel estimation for LTE uplink in high Doppler spread," in IEEE Wireless Commun. and Netw. Conf., 2008, pp. 1126–1130.
- [7] J. T. J. Penttinen, The LTE-Advanced Deployment Handbook. John Wiley & Sons, Ltd, 2016.
- [8] M. Sauter, From GSM to LTE-Advanced Pro and 5G: an introduction to mobile networks and mobile broadband. John Wiley & Sons, Ltd, 2017.
- [9] R. Irmer, H.-P. Mayer, A. Weber, V. Braun, M. Schmidt, M. Ohm, N. Ahr, A. Zoch, C. Jandura, P. Marsch et al., "Multisite field trial for LTE and advanced concepts," IEEE Commun. Mag., vol. 47, no. 2, pp. 92–98, 2009.
- [10] R. Q. Hu and Y. Qian, Heterogeneous Cellular Networks in Field Trial of LTE Technology. Wiley Telecom, 2013.
- [11] V. Buenestado, J. M. Ruiz-Aviles, M. Toril, S. Luna-Ramírez, and A. Mendo, "Analysis of throughput performance statistics for benchmarking LTE networks," IEEE Commun. Lett., vol. 18, no. 9, pp. 1607–1610, 2014.
- [12] H. A. Salman, G. Aldabbagh, Z. Taha, and L. F. Ibrahim, "Topological planning and design of heterogeneous mobile networks in dense areas," in International Conference on Computational Science and Computational Intelligence (CSCI), 2015, pp. 709–714.
- [13] M. Slanina, L. Klozar, and S. Hanus, "Practical measurement of data throughput in LTE network depending on physical layer parameters," in 24th International Conference Radioelektronika (RADIOELEKTRONIKA), 2014, pp. 1–4.
- [14] M. P. Wylie-Green and T. Svensson, "Throughput, capacity, handover and latency performance in a 3GPP LTE FDD field trial," in Global Telecommunications Conference (GLOBECOM), 2010, pp. 1–6.
- [15] J.-B. Landre, Z. El Rawas, R. Visoz, and S. Bouguermouh, "Realistic performance of LTE: In a macro-cell environment," in IEEE Vehicular Technology Conference, 2012, pp. 1–5.

- [16] B. Hagerman, K. Werner, and J. Yang, "MIMO performance at 700MHz: Field trials of LTE with handheld UE," in *IEEE Vehicular Technology Conference*, 2011, pp. 1–5.
- [17] J. Furuskog, K. Werner, M. Riback, and B. Hagerman, "Field trials of LTE with 4x4 MIMO," *Ericsson Review*, vol. 87, no. 1, pp. 10–15, 2010.
- [18] M. Lerch and M. Rupp, "Measurement-based evaluation of the LTE MIMO downlink at different antenna configurations," in *International ITG Workshop on Smart Antennas (WSA)*, 2013, pp. 1–6.
- [19] J. Erkkilä, M. Koskela, J. Heikkilä, T. Kupiainen, M. Heikkilä, T. Kipola, A. Nykanen, and R. Saukkonen, "Antenna configuration comparison in challenging NLOS locations," in *2017 European Conference on Networks and Communications (EuCNC)*, June 2017, pp. 1–5.
- [20] K. Werner, J. Furuskog, M. Riback, and B. Hagerman, "Antenna configurations for 4x4 MIMO in LTE-field measurements," in *IEEE Vehicular Technology Conference*, 2010, pp. 1–5.
- [21] M. Danneberg, J. Holfeld, M. Grieger, M. Amro, and G. Fettweis, "Field trial evaluation of UE specific antenna downtilt in an LTE downlink," in *International ITG Workshop on Smart Antennas (WSA)*, 2012, pp. 274–280.
- [22] N. Becker, A. Rizk, and M. Fidler, "A measurement study on the application-level performance of LTE," in *IFIP Networking Conference*, 2014, pp. 1–9.
- [23] J. Beyer, J. Belschner, J. Chen, O. Klein, R. Linz, J. Muller, Y. Xiang, and X. Zhao, "Performance measurement results obtained in a heterogeneous LTE field trial network," in *IEEE Vehicular Technology Conference*, 2013, pp. 1–5.
- [24] R. Merz, D. Wenger, D. Scanferla, and S. Mauron, "Performance of LTE in a high-velocity environment: a measurement study," in *Proceedings of the 4th workshop on all things cellular: operations, applications, & challenges*, 2014, pp. 47–52.
- [25] A. Brutyan, "Performance Analyses Of Different MIMO Modes In LTE Release 8 Networks," Master's thesis, Rijksuniversiteit Groningen, the Netherlands, 2013.
- [26] R. Parihar and R. Nakkeeran, "Performance analysis of LTE networks in different transmission modes using 16-QAM under fading channels," in *International Conference on Communications and Signal Processing (ICCS)*, April 2015, pp. 0979–0983.
- [27] C. F. Ball, R. Müllner, J. Lienhart, and H. Winkler, "Performance analysis of Closed and Open loop MIMO in LTE," in *European Wireless Conference (EW)*, 2009, pp. 260–265.
- [28] R. Müllner, C. F. Ball, K. Ivanov, J. Lienhart, and P. Hric, "Contrasting open-loop and closed-loop power control performance in UTRAN LTE uplink by UE trace analysis," in *IEEE International Conference on Communications (ICC)*, 2009, pp. 1–6.
- [29] J. Beyer, U. Isensee, and H. Droste, "A measurement based approach to predict the MIMO throughput of the LTE downlink in RF planning tools," in *IEEE Vehicular Technology Conference*, 2011, pp. 1–5.
- [30] J. Robson, "The LTE/SAE trial initiative: Taking LTE-SAE from specification to rollout," *IEEE Communications Magazine*, vol. 47, no. 4, pp. 82–88, 2009.
- [31] J.-B. Landre, Z. El Rawas, and R. Visoz, "LTE performance assessment Prediction versus field measurements," in *2013 IEEE 24th Annual International Symposium on Personal, Indoor, and Mobile Radio Communications (PIMRC)*, 2013, pp. 2866–2870.
- [32] P. Harris, J. Vieira, W. B. Hasan, L. Liu, S. Malkowsky, M. Beach, S. Armour, F. Tufvesson, and O. Edfors, "Achievable Rates and Training Overheads for a Measured LOS Massive MIMO Channel," *IEEE Wireless Communications Letters*, pp. 1–1, 2018.
- [33] M. Laner, P. Svoboda, P. Romirer-Maierhofer, N. Nikaein, F. Ricciato, and M. Rupp, "A comparison between one-way delays in operating HSPA and LTE networks," in *International Symposium on Modeling and Optimization in Mobile, Ad Hoc and Wireless Networks (WiOpt)*, 2012, pp. 286–292.
- [34] D. Nguyen-Thanh, T. Le-Tien, C. Bui-Thu, and T. Le-Thanh, "LTE indoor MIMO performances field measurements," in *International Conference on Advanced Technologies for Communications (ATC)*, Oct 2014, pp. 84–89.
- [35] T. Sakata, A. Yamamoto, K. Olesen, J. Å. Nielsen, and G. F. Pedersen, "MIMO throughput measurement in an urban area using a LTE mobile terminal," in *International Symposium on Antennas and Propagation (ISAP)*, Oct 2012, pp. 339–342.
- [36] V. Sevindik, J. Wang, O. Bayat, and J. Weitzen, "Performance evaluation of a real Long Term Evolution (LTE) network," in *IEEE Conference on Local Computer Networks Workshops (LCN Workshops)*, 2012, pp. 679–685.
- [37] Y. S. Ho, Y. B. Lin, J. C. Chen, H. C. H. Rao, and Y. Coral, "Voice/Video Quality Measurement for LTE Services," *IEEE Wireless Communications*, pp. 1–8, 2018.
- [38] E. Dahlman, S. Parkvall, J. Skold, and P. Beming, *3G evolution: HSPA and LTE for mobile broadband*. Academic press, 2010.
- [39] TS36.211, "3rd Generation Partnership Project, Technical Specification Group Radio Access Network: Evolved Universal Terrestrial Radio Access (E-UTRA), Physical Channels and Modulation," 3GPP, Standard.
- [40] C. Cox, *An introduction to LTE: LTE, LTE-advanced, SAE and 4G mobile communications*. John Wiley & Sons, 2012.
- [41] S. M. Alamouti, "A simple transmit diversity technique for wireless communications," *IEEE Journal on selected areas in communications*, vol. 16, no. 8, pp. 1451–1458, 1998.
- [42] J. Lee, J.-K. Han, and J. Zhang, "Mimo technologies in 3gpp lte and lte-advanced," *EURASIP J. Wirel. Commun. Netw.*, vol. 2009, pp. 3:1–3:10, Mar. 2009.
- [43] TS36.306, "3rd Generation Partnership Project; Technical Specification Group Radio Access Network; Evolved Universal Terrestrial Radio Access (E-UTRA); User Equipment (UE) radio access capabilities," 3GPP, Standard.
- [44] X. Zhang, *LTE Optimization Engineering Handbook*. Wiley-IEEE Press, 2017.
- [45] Youtube help. [Last accessed 28 September 2017]. [Online]. Available: <https://support.google.com/youtube/answer/78358?hl=en>
- [46] Netflix. Recommended internet speed. [Last accessed 28 September 2017]. [Online]. Available: <https://help.netflix.com/>
- [47] Skype Support. How much bandwidth does skype need? [Last accessed 28 September 2017]. [Online]. Available: <https://support.skype.com/>
- [48] R. Davies. 5G Network Technology: Putting Europe At The Leading Edge. [Last accessed 28 September 2017]. [Online]. Available: [http://www.europarl.europa.eu/RegData/etudes/BRIE/2016/573892/EPRS_BRI\(2016\)573892_EN.pdf](http://www.europarl.europa.eu/RegData/etudes/BRIE/2016/573892/EPRS_BRI(2016)573892_EN.pdf)
- [49] TS36.213, "3rd Generation Partnership Project, Technical Specification Group Radio Access Network: Evolved Universal Terrestrial Radio Access (E-UTRA); Physical Layer Procedures," 3GPP, Standard.
- [50] P. Ohlen, B. Skubic, A. Rostami, K. Laraqui, F. Cavaliere, B. Varga, and N. F. Lindqvist, "Flexibility in 5G transport networks the key to meeting the demand for connectivity," in *Ericsson Technology Review*, vol. 93. Ulf Evaldsson, 2016, p. 41. [Online]. Available: <https://www.ericsson.com/assets/local/publications/ericsson-technology-review/docs/2016/ericsson-technology-review-1-2016.pdf>
- [51] Huawei, "AAU5271 Description," Tech. Rep., March, 2017.



GEDIZ SEZGIN graduated from Istanbul Technical University in Electronics and Communication Engineering in 1987 and received his Master's degree from the same university in 1991 and he started pursuing PhD degree at the same university. He started his career at Alcatel Teletas with cable TV project in 1991. Mr. Sezgin joined Turkcell as Network Engineer in 1995. In October 2015 he appointed as Senior Vice President of Network Technologies under the Technology Function. Previously, he was Senior Vice President of Information and Communication Technologies, Chief Information and Communication Technologies Officer, Director of Application Operations, Director of Service Network under the ICT Function and held various executive positions.



YAGMUR COSKUN was born in Bodrum, Mugla, Turkey, in 1994. She received her B.S. degree from Istanbul Technical University, Turkey in 1994 and is currently studying for a Master's degree in telecommunications engineering in Istanbul Technical University. Her research interests are in the area of mobile communications systems such as 3G, LTE, LTE-A and also include OFDM, signal processing and physical layer based security threats.



GUNES KARABULUT KURT (M06-SM'15) received the B.S. degree (Hons.) in electronics and electrical engineering from Bogazici University, Istanbul, Turkey, in 2000, and the M.A.Sc. and Ph.D. degrees in electrical engineering from the University of Ottawa, ON, Canada, in 2002 and 2006, respectively. From 2000 to 2005, she was a Research Assistant with the CASP Group, University of Ottawa. From 2005 to 2006, she was with

TenXc Wireless, where she worked on location estimation and radio-frequency identification systems. From 2006 to 2008, she was with Edgewater Computer Systems Inc., where she worked on high-bandwidth networking in aircraft and priority-based signaling methodologies. From 2008 to 2010, she was with Turkcell Research and Development Applied Research and Technology, Istanbul. Since 2010, she has been an Associate Professor with Istanbul Technical University. Her research interests include sparse signal decomposition algorithms, multicarrier networks, traffic analysis, and network planning/management. She is a Marie Curie Fellow.



ERTUGRUL BASAR (S'09-M'13-SM'16) was born in Istanbul, Turkey, in 1985. He received his B.S. degree (Hons.) from Istanbul University, Turkey, in 2007, and his M.S. and Ph.D. degrees from Istanbul Technical University, Turkey, in 2009 and 2013, respectively. From 2011 to 2012, he was with the Department of Electrical Engineering, Princeton University, Princeton, NJ, USA, as a Visiting Research Collaborator. He is currently an Associate Professor with the Department of Electrical and Electronics Engineering, Koç University, Istanbul, Turkey.

Previously, he was an Assistant Professor and an Associate Professor with Istanbul Technical University from 2014 to 2017 and 2017 to 2018, respectively. He is an inventor of three pending/granted patents on index modulation schemes. His primary research interests include MIMO systems, index modulation, cooperative communications, OFDM, visible light communications, and signal processing for communications.

Recent recognition of his research includes the Science Academy (Turkey) Young Scientists (BAGEP) Award in 2018, Turkish Academy of Sciences Outstanding Young Scientist (TUBA-GEBIP) Award in 2017, the first-ever IEEE Turkey Research Encouragement Award in 2017, and the Istanbul Technical University Best Ph.D. Thesis Award in 2014. He is also the recipient of five Best Paper Awards including one from the IEEE International Conference on Communications 2016. He has served as a TPC track chair or a TPC member for several IEEE conferences including GLOBECOM, VTC, PIMRC, and so on. Dr. Basar currently serves as an Editor of the IEEE Transactions on Communications and *Physical Communication* (Elsevier), and as an Associate Editor of the IEEE Communications Letters. He has served as an Associate Editor for the IEEE Access from 2016 to 2018.

...